

Investigation of maximum proton energy for qualified ground-based evaluation of single-event effects in SRAM devices

Zhan-Gang Zhang¹ · Yun Huang¹ · Yun-Fei En¹ · Zhi-Feng Lei¹

Received: 10 February 2018 / Revised: 19 August 2018 / Accepted: 21 August 2018 / Published online: 14 February 2019
© China Science Publishing & Media Ltd. (Science Press), Shanghai Institute of Applied Physics, the Chinese Academy of Sciences, Chinese Nuclear Society and Springer Nature Singapore Pte Ltd. 2019

Abstract Existing standards show a clear discrepancy in the specification of the maximum proton energy for qualified ground-based evaluation of single-event effects, which can range from 180 to 500 MeV. This work finds that the threshold linear energy transfer of a tested device is a critical parameter for determining the maximum proton energy. The inner mechanisms are further revealed. High-energy deposition events (> 10 MeV) in sensitive volumes are attributed to the interaction between protons and the tungsten vias in the metallization layers.

Keywords Proton · Single-event effect · Threshold LET · Monte Carlo simulation

1 Introduction

As a major reliability factor in space-borne microelectronics [1], single-event effects (SEEs) are caused by heavy ions or protons in space radiation environment. With a higher flux than heavy ions, protons are capable of inducing SEEs through both direct and indirect ionization. SEEs

from proton direct ionization have been observed in advanced technologies (below 100 nm) primarily at proton energies below 5 MeV and have received widespread attention in recent years [2–8].

On the other hand, many studies have been published in recent years concerning SEEs from proton indirect ionization, focusing mainly on investigating proton testing methods [9, 10], proton energy effects [11], Monte Carlo simulations [12–15], and relations between proton and heavy ion SEE data [12, 15–18]. In addition, several standards have been developed in recent decades to guide ground-based testing. Some of these standards specify requirements on the proton energy range for qualified SEE evaluation. For example, in 2002 the European Space Components Coordination (ESCC) basic specification No. 25100 stated that the accelerator should be capable of delivering protons in the energy range of 20 to 200 MeV [19]. The Sandia National Laboratories document SAND 2008-6983P claimed that the radiation source must be capable of providing protons with energies over a range from at least 20 to 180 MeV. Ideally, the radiation source should be capable of producing protons with energies as high as the maximum energy of protons in the system environment [20]. For trapped protons in space, this is 400 MeV [21]. More recently, JESD234, issued in 2013, suggested that for a nondestructive single-event upset (SEU) test, testing above 200 MeV is not considered necessary. However, for single-event latchup (SEL), where some systems forbid parts with any realizable SEL cross section, testing to energies of 40–500 MeV may be necessary [22]. It can be observed that existing standards exhibit a clear discrepancy in the specification of the maximum proton energy for qualified ground-based SEE evaluation. In addition, with the constant downscaling of

This work was supported by the National Natural Science Foundation of China (No. 11505033), the Science and Technology Research Project of Guangdong, China (Nos. 2015B090901048 and 2017B090901068), and the Science and Technology Plan Project of Guangzhou, China (No. 201707010186).

✉ Zhan-Gang Zhang
zhangangzhang@163.com

¹ Science and Technology on Reliability Physics and Application of Electronic Component Laboratory, China Electronic Product Reliability and Environmental Testing Research Institute, Guangzhou 510610, China

technology, new materials, processes, and structures are being employed in modern microelectronics, which may lead to changes in the traditional maximum proton energy. Determining the maximum proton energy for qualified SEE testing may benefit the community by (1) avoiding underestimations of SEE sensitivity through using protons with unqualified energies; (2) enabling low-energy proton accelerators qualified for complete ground-based SEE tests in certain circumstances, which will reduce costs and increase the number of suitable facilities; and (3) guiding proton energy selection for in-construction proton facilities and terminals. However, limited data have been published relating to the physical nature of the maximum proton energy and the underlying mechanisms.

Thus, this study focuses on an in-depth investigation of the maximum proton energy for qualified accelerator-based SEE evaluation. Typical SRAM devices were selected, with heavy metal materials [e.g., tungsten (W) and titanium (Ti)] residing in close proximity to the sensitive volume (SV). By comparing the energy deposition spectrums in SV and SEE cross sections for protons with different energies (ranging from tens of MeV to 500 MeV), the maximum proton energy can be determined for different kinds of SRAM devices with various threshold LETs (LET_{th}). The inner mechanisms were further revealed by analyzing the impact of the top metallization layers, especially high-Z materials (W, Ti, and so on). It was found that the threshold LET for a device is a critical parameter for the determination of the maximum proton energy.

2 Analysis of space proton spectrum

As an example, Fig. 1 depicts the particle flux–energy spectrum on International Space Station (ISS, 500 km, 51.6°) orbit. The CREME96 model was employed to calculate the space particle spectrum [23, 24]. The AP8MIN model was utilized for trapped protons. The magnetic

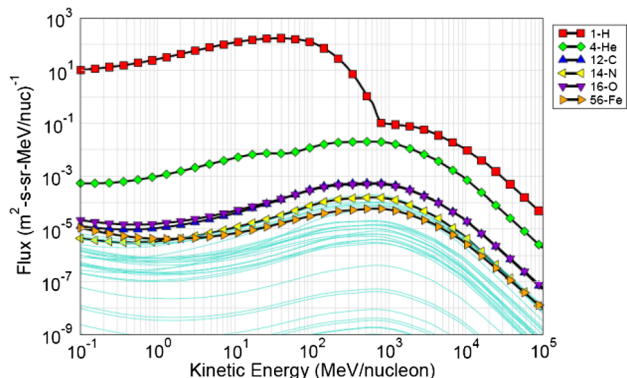


Fig. 1 (Color online) Particle flux–energy spectrum on ISS orbit (calculation conditions: solar minimum, 3-mm Al shielding)

weather condition was set as “magnetic quiet”. The space weather is solar minimum, with 3-mm Al shielding. Particles including protons, alpha particles, and heavy ions are present. It can be seen that (a) compared to other particles, the proton flux is higher; (b) trapped protons contribute to an obvious increase in the proton flux in the energy range of below several hundred MeV, and the flux of trapped protons reaches its maximum at an energy of 40 MeV; and (c) the proton flux decreases rapidly with increasing energy.

Proton energy is the primary variable in ground-based evaluation of single-event effects. However, the energies utilized in a test do not necessarily reflect the proton spectrum in space. The limits of the test energy range versus the actual environment must be taken into consideration during data analysis.

3 Monte Carlo (MC) simulations

The technology evaluated in this study consists of a typical 4 Mbit, 3.3 V CMOS SRAM [25, 26]. The 3D device model is presented in Fig. 2. A rectangular parallelepiped (RPP)-shaped SV of $2.00 \times 2.00 \times 2.25 \mu\text{m}^3$, suitable for the MC simulations, is constructed. The $4\text{-}\mu\text{m}^2$ surface of the SV is centrally located beneath the top metallization layers with respect to the beam direction. The surface area of the device model is $10 \times 10 \mu\text{m}^2$, which is considered sufficiently large to include the impact of all surrounding protons. Note that although only one memory cell is constructed, the charge-sharing effects between cells were indirectly included in the MC calculations. The reasons for this are described as follows. During the simulations, all the protons were normally and uniformly incident at the surface of the device model, and all the energy

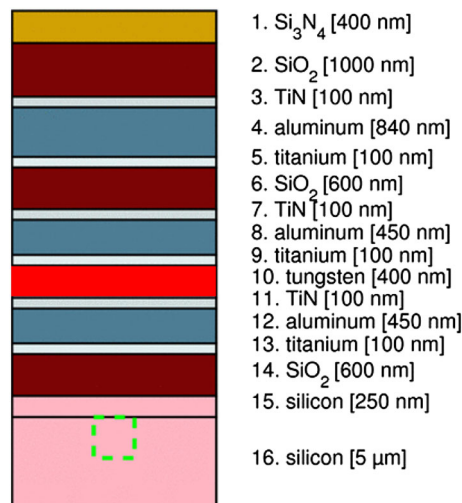


Fig. 2 (Color online) The device model (not to scale)

depositions in the central SV induced by incident protons were recorded. For protons striking the surrounding area of the central single SV, their energy depositions in the central SV induced by either direct or indirect ionization were also taken into account. However, protons striking the surrounding area of the central single SV will bombard other SVs close to the central one, which means that charge sharing between nearby SVs was indirectly considered.

Furthermore, to investigate the proton energy effect on destructive SEEs, the depth of the constructed SV was expanded to 30 μm , because some CMOS devices may have sensitive volume depths of 30 μm or more. Accordingly, the device model in Fig. 2 was modified to fit the change in SV depth. Specifically, the depth of the substrate silicon layer was changed to 50 μm . After the simulations, the SEE responses of the two SVs were compared.

The Geant4 [27] and CRÈME-MC [23, 24, 28, 29] toolkits were utilized. For most of the simulation runs, the ion fluence was between 10^{12} and 10^{14} p/cm^2 , allowing for sufficient statistics. Direct ionization and detailed nuclear reaction processes were both computed, excluding the details of δ -rays. After each run, the deposited energy spectrums in the SV and cross sections were extracted and analyzed.

4 Results and analysis

4.1 Energy dependence

Figures 3 and 4 present the spectrums of the deposited energy in the device SVs with depths of 2.25 μm and 30 μm , respectively. Protons with various energies, ranging

from 20 to 500 MeV, were utilized. The energy points were chosen based on existing test standards including ESCC 25100, SAND 2008-6983P, and JESD234. It can be observed that the spectrums exhibit a wide distribution of energy deposition, resulting from both direct and indirect ionization. The left peaks in Figs. 3 and 4 are caused by proton direct ionization. As the proton energy increases, the left peak moves toward the low-deposited-energy side, resulting from a decrease in the electric stopping power of protons.

Conversely, the opposite trend is observed on the high-deposited-energy side, marked by red dashed circles in Figs. 3 and 4.

(1) In Fig. 3, for the 20 MeV protons the maximum deposited energy in the SV is only around 4 MeV. This value increases for protons with higher energies. For the 500 MeV protons, the maximum event can reach as high as 20 MeV. The equivalent LET for proton-induced secondary recoils can be calculated as follows:

$$\text{LET}_{\text{EQ}} = \frac{E_d}{R_{\text{SV}} \times \rho_{\text{Si}}}.$$

Here, LET_{EQ} represents the equivalent LET of proton recoils in the SV, as defined by R. Ladbury in 2015 [16], E_d denotes the deposited energy of secondary recoils in the SV, and R_{SV} denotes the travel distance of secondary recoils in the SV. After a nuclear reaction process with a DUT nucleus, proton-induced secondary recoils can strike the SV from all directions. To determine the minimum LET_{EQ} value of this maximum event, the largest R_{SV} , i.e., the diagonal incidence, should be utilized. Consequently, it can be concluded that the maximum LET of secondary

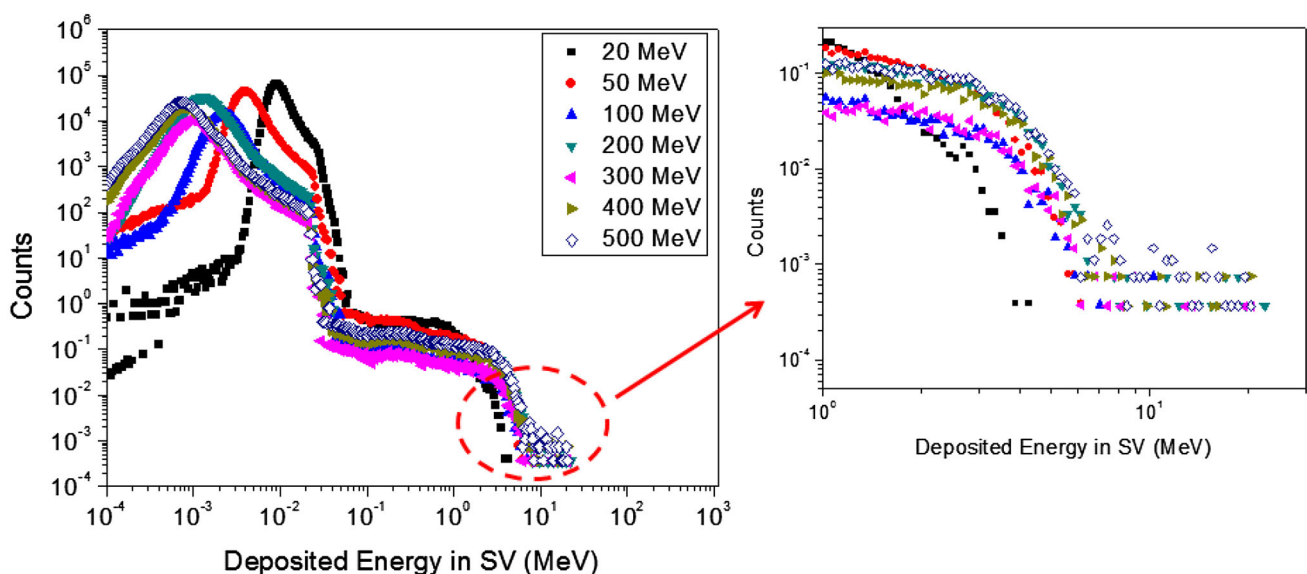


Fig. 3 (Color online) Spectrums of deposited energy in the device SV with a depth of 2.25 μm , for protons with various energies

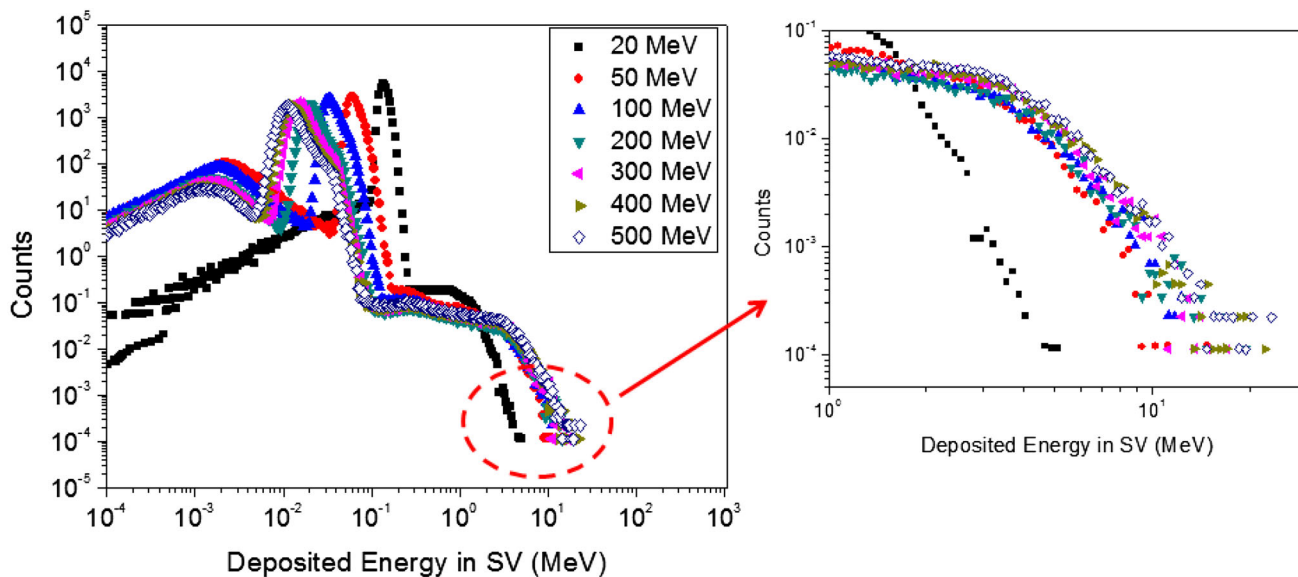


Fig. 4 (Color online) Spectrums of deposited energy in the device SV with depth of 30 μm, for protons with various energies

recoils induced by 500 MeV protons in the device should be no less than 24 MeV cm²/mg.

(2) In Fig. 4, a similar trend is observed as in Fig. 3, which verifies the proton energy effect in devices with different sensitive volumes.

By reverse integrating the counts of energy deposition events (see Figs. 3 and 4) divided by the ion fluence, the cross section can be obtained as a function of the critical energy (see Figs. 5 and 6) as

$$\sigma = \frac{\int_{E_c} N(E_d)}{F},$$

where σ represents the cross section, E_c denotes the critical energy of the device SV, N denotes the count of energy deposition events in Figs. 3 and 4, and F is the ion fluence per cm².

By comparing Figs. 5 and 6, it can be observed that (1) the trends of the proton energy effect on the SEE response are similar and (2) the proton-induced cross sections of the device with an SV depth of 30 μm are higher by approximately one order of magnitude in comparison with those of the device with an SV depth of 2.25 μm.

By determining the critical energy in Fig. 5, the plot of the SEU cross section against the proton energy, which is

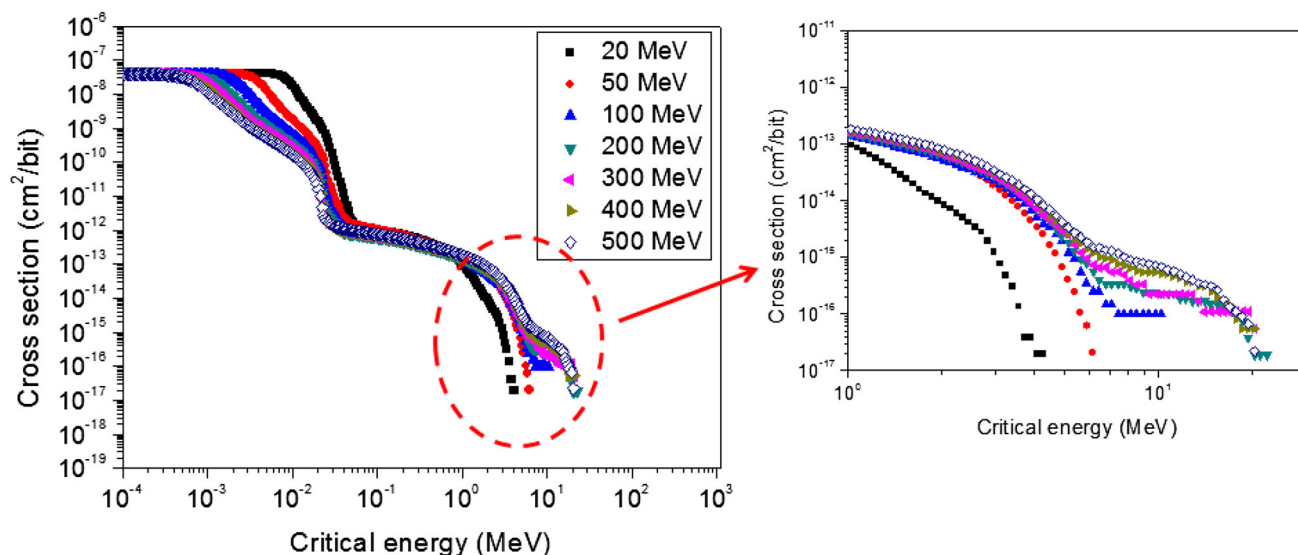


Fig. 5 (Color online) SEU cross section as a function of the critical energy for the device SV with a depth of 2.25 μm for protons with various energies

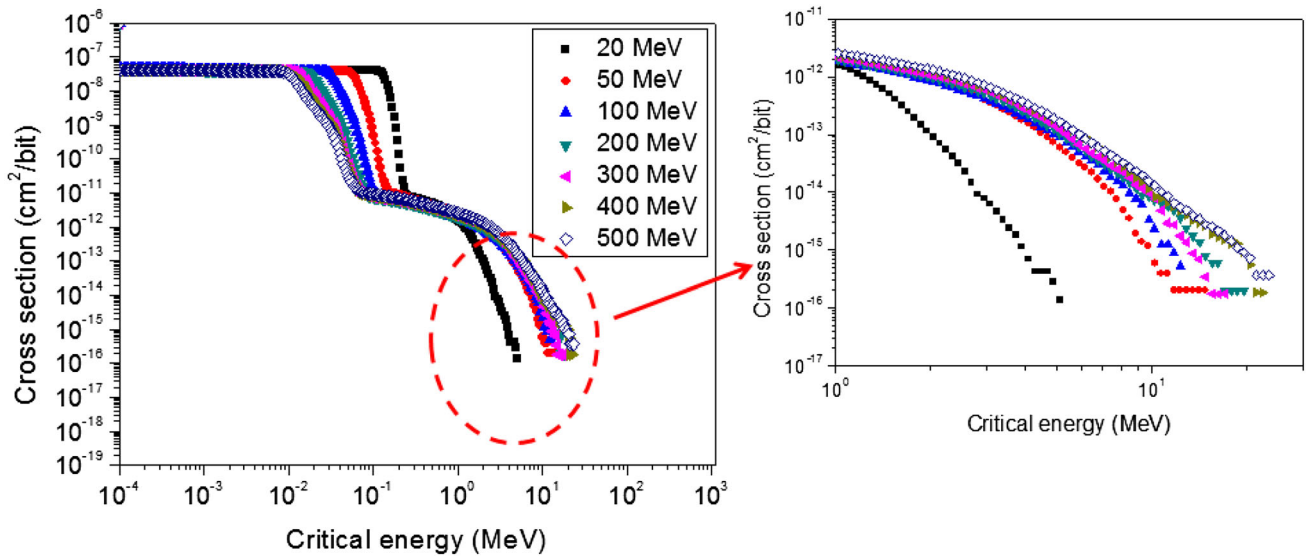


Fig. 6 (Color online) SEU cross section as a function of the critical energy for the device SV with a depth of 30 μm for protons with various energies

usually the end product of accelerator-based SEE testing, can be obtained (as shown in Fig. 7). The threshold LET in the plot is calculated as:

$$LET_{th} = \frac{E_c}{D_{SV} \times \rho_{Si}}$$

Here, D_{SV} represents the depth of the device SV.

In Fig. 7, for a small LET_{th} of 1 MeV cm²/mg the SEU cross section appears to be constant, even for a proton energy of 20 MeV. With an increase in LET_{th} to 4 MeV cm²/mg, the SEU cross section is saturated at a proton energy of 50 MeV. As the LET_{th} increases further, the SEU cross section appears to increase constantly by several orders of magnitude as the proton energy increases

to 500 MeV. Another notable phenomenon is that as the LET_{th} increases above 8 MeV cm²/mg, the SEU cross section– E_p curve becomes “shorter.” Protons with an energy below 200 MeV cannot induce SEU when LET_{th} is below 20 MeV cm²/mg. In Fig. 8, a similar trend is observed as in Fig. 7, which verifies the threshold LET effect in devices with different sensitive volumes. Note that in Fig. 8, the critical energy rather than the threshold LET is used to define the device SEE sensitivity. The reason for this is that for the device with an SV depth of 30 μm, the relation between the critical energy and threshold LET can change, given that proton-induced secondary particles can penetrate through the device SV from all directions, and

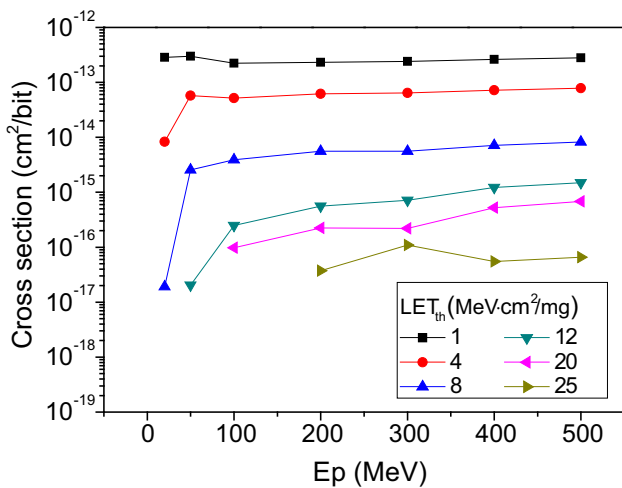


Fig. 7 (Color online) Plot of proton-induced SEU cross section against proton energy under various device threshold LETs. The depth of the device SV is 2.25 μm

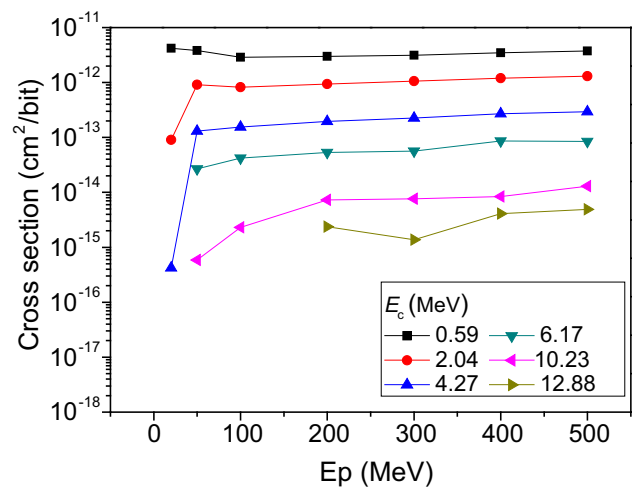


Fig. 8 (Color online) Plot of proton-induced SEU cross section against proton energy under various device critical energies. The depth of the device SV is 30 μm

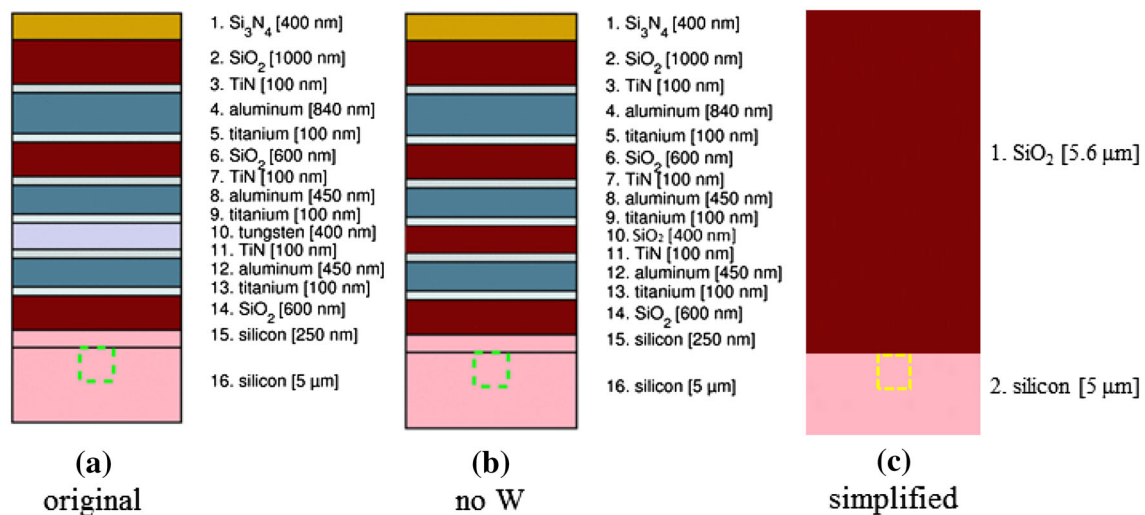


Fig. 9 (Color online) Illustration of the change in the device model: **a** original, **b** "no W" represents the result of a W via layer replaced by a silica layer, **c** "simplified" represents the result of all metallization layers replaced by silica layers (not to scale)

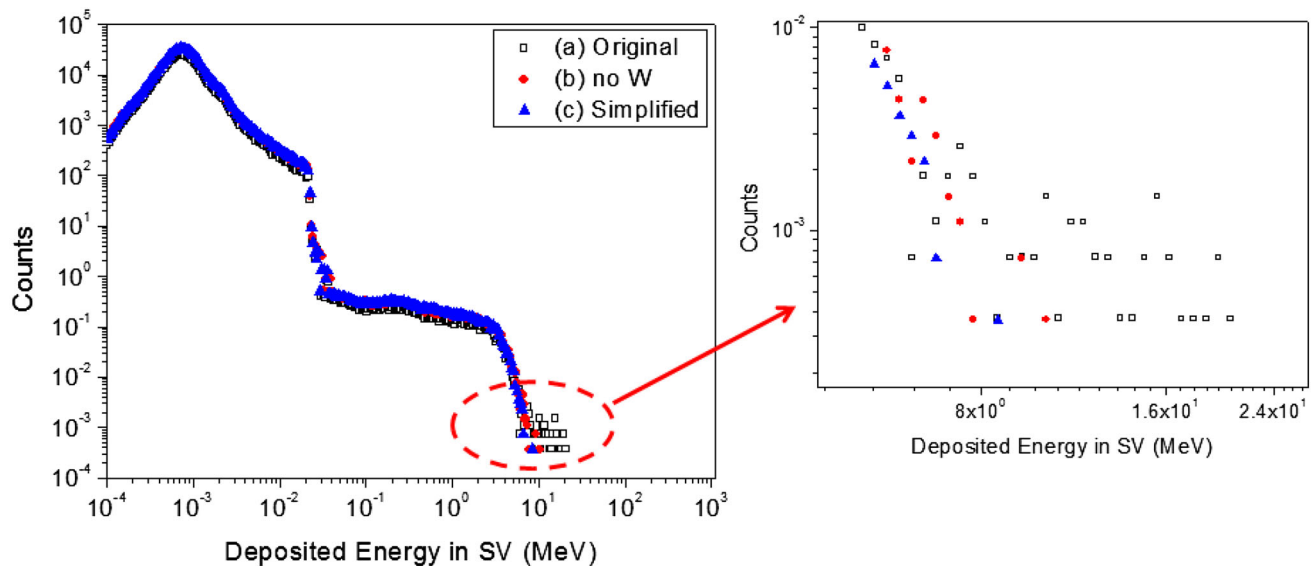


Fig. 10 (Color online) Spectrums of deposited energy for 500 MeV protons in the device SV with a depth of 2.25 μm. Three cases are compared: original, no W, and simplified

the resulting path lengths in the device SV can be very different.

Thus, it can be concluded that the threshold LET is an important parameter in determining the curve shape and maximum proton energy. For electronic devices with a low-threshold LET, which are usually unhardened, testing under 200 MeV is sufficient. However, for high-threshold LET devices, which are usually hardened, tests using insufficient energy may (1) underestimate the saturated cross section and thus the device sensitivity and (2) miss the resulting effects, which may lead to catastrophic consequences owing to incorrect immunity results.

4.2 Metallization dependence

To further investigate the mechanisms of proton-induced SEE, especially the impact of high-Z materials in the metallization layers, the device model used in the MC simulations was modified by replacing the W via layer by silica or replacing all the metallization layers by silica (see Fig. 9). By comparing the simulation results, the metallization dependence can be distinguished and quantitatively analyzed.

Figure 10 depicts the spectrums of deposited energy for 500 MeV protons in the device SV. Three cases are

compared: original, no W, and simplified. By comparing (a) original and (b) no W, we observe that high-energy deposition events (> 10 MeV) result from interactions between the 500 MeV protons and W. It appears that changing the metallization layers has no impact on the deposited energy spectrum in the low-energy region (< 10 MeV), which is thus attributed to the interaction between protons and Si and O elements, including direct and indirect ionization processes.

5 Conclusion

In this work, the maximum proton energy for qualified earth-based SEE testing is investigated using Monte Carlo simulations for SRAM devices with various threshold LETs. The deposited energy spectrums for protons in the device SV and the cross sections are obtained and analyzed. The maximum deposited energy in the SV increases for protons with higher energies, along with the generation probability. For 500 MeV protons, the maximum event can reach as high as 20 MeV. It is found that the threshold LET of DUT is an important parameter for determining the $\sigma \sim E_p$ curve shape and maximum proton energy. For high-threshold LET devices, which are usually hardened, tests using insufficient energy may (1) underestimate the saturated cross section and thus the device sensitivity and (2) miss the resulting effects, which may lead to catastrophic consequences owing to incorrect immunity results. Finally, the mechanisms of proton-induced SEE are further revealed, showing that high-energy deposition events (> 10 MeV) in the SV result from interactions between 500 MeV protons and W. It appears that changing the metallization layers has no impact on the deposited energy spectrum in the low-energy region (< 10 MeV), which is thus attributed to the interaction between protons and Si and O elements, including direct and indirect ionization processes.

Acknowledgement The authors would like to thank the CRÈME-96, CRÈME-MC, and Geant4 groups, and also Vanderbilt University for support of the CRÈME software.

References

1. P.E. Dodd, M.R. Shaneyfelt, J.R. Schwank et al., Current and future challenges in radiation effects on CMOS electronics. *IEEE Trans. Nucl. Sci.* **57**, 1747–1763 (2010). <https://doi.org/10.1109/TNS.2010.2042613>
2. K.P. Rodbell, D.F. Heidel, H.H.K. Tang et al., Low-energy proton-induced single-event-upsets in 65 nm node, silicon-on-insulator, latches and memory cells. *IEEE Trans. Nucl. Sci.* **54**, 2474–2479 (2007). <https://doi.org/10.1109/TNS.2007.909845>
3. D.F. Heidel, P.W. Marshall, K.A. LaBel et al., Low energy proton single-event-upset test results on 65 nm SOI SRAM. *IEEE Trans. Nucl. Sci.* **55**, 3394–3400 (2008). <https://doi.org/10.1109/TNS.2008.2005499>
4. D.F. Heidel, P.W. Marshall, J.A. Pellish et al., Single-event upsets and multiple-bit upsets on a 45 nm SOI SRAM. *IEEE Trans. Nucl. Sci.* **56**, 3499–3504 (2009). <https://doi.org/10.1109/TNS.2009.2033796>
5. B.D. Sierawski, J.A. Pellish, R.A. Reed et al., Impact of low-energy proton induced upsets on test methods and rate predictions. *IEEE Trans. Nucl. Sci.* **56**, 3085–3092 (2009). <https://doi.org/10.1109/TNS.2009.2032545>
6. R.K. Lawrence, J.F. Ross, N.F. Haddad et al., in *Soft Error Sensitivities in 90 nm Bulk CMOS SRAMs*. 2009 IEEE Radiation Effects Data Workshop, Quebec City, QC, Canada, 20–24 July 2009, pp. 123–126. <https://doi.org/10.1109/redw.2009.5336302>
7. E.H. Cannon, M. Cabanas-Holmen, J. Wert et al., Heavy ion, high-energy, and low-energy proton SEE sensitivity of 90-nm RHBD SRAMs. *IEEE Trans. Nucl. Sci.* **57**, 3493–3499 (2010). <https://doi.org/10.1109/TNS.2010.2086482>
8. N.F. Haddad, A.T. Kelly, R.K. Lawrence et al., Incremental enhancement of SEU hardened 90 nm CMOS memory cell. *IEEE Trans. Nucl. Sci.* **58**, 975–980 (2011). <https://doi.org/10.1109/TNS.2011.2128882>
9. J.R. Schwank, M.R. Shaneyfelt, P.E. Dodd, Radiation hardness assurance testing of microelectronic devices and integrated circuits: radiation environments, physical mechanisms, and foundations for hardness assurance. *IEEE Trans. Nucl. Sci.* **60**, 2074–2100 (2013). <https://doi.org/10.1109/TNS.2013.2254722>
10. J.R. Schwank, M.R. Shaneyfelt, P.E. Dodd, Radiation hardness assurance testing of microelectronic devices and integrated circuits: test guideline for proton and heavy ion single-event effects. *IEEE Trans. Nucl. Sci.* **60**, 2101–2118 (2013). <https://doi.org/10.1109/TNS.2013.2261317>
11. J.R. Schwank, M.R. Shaneyfelt, J. Baggio et al., Effects of particle energy on proton-induced single-event latchup. *IEEE Trans. Nucl. Sci.* **52**, 2622–2629 (2005). <https://doi.org/10.1109/TNS.2005.860672>
12. P.M. O'Neill, G.D. Badhwar, W.X. Culpepper, Risk assessment for heavy ions of parts tested with protons. *IEEE Trans. Nucl. Sci.* **44**, 2311–2314 (1997). <https://doi.org/10.1109/23.659052>
13. P.M. O'Neill, G.D. Badhwar, W.X. Culpepper, Internuclear cascade-evaporation model for LET spectra of 200 MeV protons used for parts testing. *IEEE Trans. Nucl. Sci.* **45**, 2467–2474 (1998). <https://doi.org/10.1109/23.736487>
14. D.M. Hiemstra, E.W. Blackmore, LET spectra of proton energy levels from 50 to 500 MeV and their effectiveness for single event effects characterization of microelectronics. *IEEE Trans. Nucl. Sci.* **50**, 2245–2250 (2003). <https://doi.org/10.1109/TNS.2003.821811>
15. C.C. Foster, P.M. O'Neill, C.K. Kouba, Risk assessment based on upset rates from high energy proton tests and Monte Carlo simulations. *IEEE Trans. Nucl. Sci.* **55**, 2962–2969 (2008). <https://doi.org/10.1109/TNS.2008.2008185>
16. R.L. Ladbury, J.M. Lauenstein, K.P. Hayes, Use of proton SEE data as a proxy for bounding heavy-ion SEE susceptibility. *IEEE Trans. Nucl. Sci.* **62**, 2505–2510 (2015). <https://doi.org/10.1109/TNS.2015.2496351>
17. R.L. Ladbury, J.M. Lauenstein, Evaluating constraints on heavy-ion SEE susceptibility imposed by proton SEE testing and other mixed environments. *IEEE Trans. Nucl. Sci.* **64**, 301–308 (2017). <https://doi.org/10.1109/TNS.2016.2640948>
18. R.G. Alía, M. Brugger, E. Daly et al., Simplified SEE sensitivity screening for COTS components in space. *IEEE Trans. Nucl. Sci.* **64**, 882–890 (2017). <https://doi.org/10.1109/TNS.2017.2653863>

19. ESCC Basic Specification 25100, Single event effects test method and guidelines (2002)
20. Sandia National Laboratories Document SAND 2008-6983P, Radiation hardness assurance testing of microelectronic devices and integrated circuits: Test guideline for proton and heavy ion single-event effects (2008)
21. E.G. Stassinopoulos, J.P. Raymond, The space radiation environment for electronics. *Proc. IEEE* **76**, 1423–1442 (1988). <https://doi.org/10.1109/5.90113>
22. JESD234, Test standard for the measurement of proton radiation single event effects in electronic devices (2013)
23. A.J. Tylka, J.H. Adams, P.R. Boberg et al., CREME96: a revision of the cosmic ray effects on micro-electronics code. *IEEE Trans. Nucl. Sci.* **44**, 2150–2160 (1997)
24. <https://creme.isde.vanderbilt.edu/>
25. K.M. Warren, R.A. Weller, M.H. Mendenhall et al., The contribution of nuclear reactions to heavy ion single event upset cross-section measurements in a high-density SEU hardened SRAM. *IEEE Trans. Nucl. Sci.* **52**, 2125–2131 (2005). <https://doi.org/10.1109/TNS.2005.860677>
26. R.A. Reed, R.A. Weller, M.H. Mendenhall et al., Impact of ion energy and species on single event effects analysis. *IEEE Trans. Nucl. Sci.* **54**, 2312–2321 (2007). <https://doi.org/10.1109/TNS.2007.909901>
27. S. Agostinelli, J. Allison, K. Amako et al., GEANT4—a simulation toolkit. *Nucl. Instrum. Methods Phys. Res. A* **506**, 250–303 (2003). [https://doi.org/10.1016/S0168-9002\(03\)01368-8](https://doi.org/10.1016/S0168-9002(03)01368-8)
28. R.A. Weller, M.H. Mendenhall, R.A. Reed et al., Monte Carlo simulation of single event effects. *IEEE Trans. Nucl. Sci.* **57**, 1726–1746 (2010). <https://doi.org/10.1109/TNS.2010.2044807>
29. J.H. Adams, A.F. Barghouty, M.H. Mendenhall et al., CRÈME: the 2011 revision of the cosmic ray effects on micro-electronics code. *IEEE Trans. Nucl. Sci.* **59**, 3141–3147 (2012). <https://doi.org/10.1109/TNS.2012.2218831>